Supporting Information

Naci et al. 10.1073/pnas.1407007111

SI Methods

Patients' Narrative Clinical Histories. Patient 1 (female; 20 y old) suffered the onset of progressive encephalopathy of unknown etiology in April 2007. Subsequent MRI scans revealed generalized cerebral and cerebellar volume loss with hyperintensities over the frontal lobes and attenuation of the distal arterial branches. Progressive cognitive deterioration that culminated in complete loss of behavioral responsivity ensued. Since July 2009 the patient has received palliative care in the home setting. In five behavioral assessments conducted by the research team in the 3 mo before the functional magnetic resonance imaging (fMRI) testing the patient scored 4–8 (out of a maximum of 23) in the JFK Coma Recovery Scale (CRS-R) (1) and received a diagnosis of either vegetative state (VS) or minimally conscious state (MCS) when visual pursuit could be detected. When admitted for fMRI testing 68 mo postinjury, the patient scored 8/23 and received a diagnosis of MCS. (CRS-R subscores on the day of fMRI testing: auditory, 1—startle; visual, 3—visual pursuit; motor, 1—abnormal posturing; oromotor/verbal, 1—oral reflexive movement; communication, none; arousal:, 2—eye opening w/o stimulation.)

Patient 2 (male; 34 y old) suffered a cardiac arrest from being kicked in the chest in August 1997. The hypoxic event led to secondary hypoxic ischemic encephalopathy with multiple neurological deficits. After a 3-wk coma the patient received a diagnosis of VS and was discharged to a long-term care facility. In six behavioral assessments conducted by the research team in the 3 mo before the fMRI testing the patient scored 6–10 (out of a maximum of 23) in the CRS-R scale and received a diagnosis of either VS or MCS when visual pursuit could be detected. When admitted for fMRI testing 184 mo postinjury, the patient scored 9/23 and received a diagnosis of MCS. (CRS-R subscores on the day of fMRI testing: auditory, 1—startle; visual, 3—visual pursuit; motor, 2—flexion withdrawal; oromotor/verbal, 1—oral reflexive movement; communication, none; arousal, 2—eye opening w/o stimulation.)

Stimuli and Design. ***Experiment 1.*** The edited Hitchcock movie depicted a 5-y-old boy who finds his uncle's revolver, partially loads it with bullets, and plays with it at home and in public, unaware of its power and danger. It was chosen for its age/sex neutrality, wide-ranging appeal, and engaging plot. Moreover, a longer version of this movie has been found to elicit robust brain activity, synchronized across healthy participants. To keep the scanning session brief, the movie was shortened to 8 min by editing scenes while maintaining the primary storyline. The short movie was broken down into smaller (1 s) audiovisual segments in the iMovie software (www.apple.com/ca/support/mac-apps/imovie/) to create the scrambled movie condition. The segments were arranged in pseudorandom order to avoid any movie narrative within nearby segments. Written feedback at the end of the scanning session confirmed that participants had not been able to uncover a storyline in the scrambled movie or relate it to stored knowledge of previous movies they had seen.

Experiment 2. The dual-task framework has been extensively used to investigate executive performance, as it recruits executive function for the allocation and coordination of attentional resources (2). This framework assumes that because executive function is a finite resource, in moments when the load on one executively demanding task (i.e., the movie) is greatest, the performance of a second executively demanding task will be impaired, yielding a direct, quantitative measure of the executive demands of the first task across time. The dual task in this study consisted of simultaneous performance of the Sustained Attention to Response Task (SART)—which measures sustained attention and quantifies executive function (3) —and movie viewing. SART was an optimal choice of an executively demanding task that could be performed while simultaneously watching the movie. SART operates on the principle that insufficient attention to a task can result in slips of action as automatic, unintended action sequences are triggered inappropriately. These automatic actions result in performance errors that can be detected in the SART reaction times. Specifically, in the SART, participants are required to respond with a button press to a series of randomly presented ("go") digits but withhold responses to one prespecified ("no go") digit. A signature of the SART is that a shortening of reaction times indicates a decrement in executive control or, conversely, an increment in response automaticity (3–5). In particular, a shortening of reaction time predicts an increased likelihood of a subsequent incorrect response to a "no go" digit and correlates with electrophysiological measures of waning attention (6).

At the end of the dual task, participants answered 14 multiple-choice questions by selecting one of four answer options. These assessed each participant's encoding of basic facts about the movie and therefore, indirectly, their overall attention to the movie throughout its duration, as they simultaneously performed the SART. These questions and the answer options were (1) What are the boys standing behind when they shoot their toy guns? (Answers: Tree/Bush/House/Fence); (2) What kind of hat is the boy wearing throughout the movie? (Answers: Baseball Cap/Private Hat/Cowboy Hat/Newsboy Hat); (3) What does the boy find in the uncle's luggage when he's unpacking? (Answers: Knife/Baseball/New hat/Real gun); (4) Which toy animal does the boy ride in front of the supermarket? (Answers: Cow/Elephant/Unicorn/Horse); (5) What does the supermarket clerk tell the boy to do? (Answers: Feed the meter/Get off/Find your parents/Be careful); (6) When the boy is on the ride, what does he drop on the ground? (Answers: Dimes/Bullet/Gun/Hat); (7) What does the girl's father give the boy to get him to get off the ride? (Answers: Lollipop/Money/Chocolate/Nothing); (8) What reason does the boy give for not getting off the ride? (Answers: He paid for it/It was his/He got there first/He wanted to play); (9) What is the maid's name? (Answers: Mary/Jackie/Cleo/Susan); (10) What breaks when the boy shoots the gun at the end? (Answers: Statue/Mirror/Mask/Picture Frame); (11) The father is holding the gun at the end of the movie; what is the uncle holding? (Answers: Mask/Glass of wine/His hat/The bullet); (12) What is the boy standing behind when he shoots the gun at the end? (Answers: Door frame/Kitchen table/Dinning room chair/Couch); (13) What is the supermarket clerk pushing when the boy is on the ride? (Answers: Milk crates/Shopping carts/A floor display/Cart full of apples); (14) Who does the boy run toward at the end, after shooting the gun? (The maid/The father/The mother/The uncle).

Data Acquisition and Model-Driven Analysis of fMRI Time Series. ***Healthy participants.*** Participants lay supine in the scanner looking upward into a mirror box that allowed them to see a projection screen behind their head. Noise cancellation headphones (Sensimetrics, S14; www.sens.com) were used for sound delivery. Functional echo-planar images were acquired [33 slices, voxel size: 3 × 3 × 3, interslice gap of 25%, repetition time = 2,000 ms, echo time (TE) = 30 ms, matrix size = 64 × 64, flip angle (FA) = 75 degrees]. The movie, resting state, and scrambled movie scans had 246, 256, and 238 scans, respectively. An anatomical volume was obtained using a T1-weighted 3D magnetization prepared rapid acquisition gradient echo (MPRAGE) sequence (32 channel coil, voxel size: 1 × 1 × 1 mm, TA = 5 min and 38 s, TE = 4.25 ms, matrix size = 240 × 256 × 192, FA = 9 degrees). The imaging data were preprocessed and analyzed using statistical parametric mapping 8 (SPM8) (Wellcome Institute of Cognitive Neurology, www.fil.ion.ucl.ac.uk/spm/software/spm8/) and the automatic analysis pipeline software (www.cusacklab.org). The processing steps were correction for timing of slice acquisition, motion correction, normalization to a template brain, and smoothing. The data were smoothed with a Gaussian smoothing kernel of 10 mm FWHM (7). Spatial normalization was performed using SPM8's segment-and-normalize procedure, whereby the T1 structural was segmented into gray and white matter and normalized to a segmented Montreal Neurological Institute-152 template. These normalization parameters were then applied to all echo plannar images. The time series in each voxel was high-pass–filtered with a cutoff of 1/128 Hz to remove low-frequency noise and scaled to a grand mean of 100 across voxels and scans in each session. The preprocessed data were analyzed in SPM8 using the general linear model. Before analyses, the first five scans of each session were discarded to achieve T1 equilibrium and to allow participants to adjust to the noise of the scanner. Group-level correlational analyses explored, for each voxel, the cross-subject synchronization in brain activity by measuring the correlation of each subject's time course with the mean time course of all other subjects.

Brain-injured patients. Patient scanning was performed using the same 3 Tesla Siemens Tim Trio system, 32-channel head coil, and data acquisition parameters as for the healthy participants. Both patients maintained continuous spontaneous eye opening during the movie conditions, as monitored with an infrared camera placed inside the scanner. The same data preprocessing procedures as for healthy participants were applied to patient data.

Data-Driven Analyses of fMRI Time Series. Independent component analysis (ICA) is especially suited for exploring the neural dynamics from naturalistic stimulation, such as during movie viewing, where complex interactions between several stimulus factors modulate the brain activity (8), and it is not possible, without making a large number of assumptions, to create a model of the variables that drive the brain signal. As a data-driven method, ICA can reveal complex neural dynamics in the absence of a temporal model by dividing the fMRI signal into statistically independent components. Each component has a time course that describes its activity peaks and dips over the stimulus duration and a spatial distribution, which describes the brain regions that generate this activity time course. Thus, ICA can be used to reveal spatially or temporally independent parts of the fMRI signal that represent different sensory and cognitive processes within functional subsystems of the brain.

We performed Tensor ICA, a method that derives spatially orthogonal components, whose spatial and temporal features are similar across subjects. The Melodic software (http://fsl.fmrib.ox.ac.uk/fsl/fslwiki/MELODIC) was used to perform ICA with a 20-component cutoff (9). Initially, group-level analysis was performed to test whether the widespread cross-subject synchronization pattern observed during movie viewing could be separated into functionally specific spatiotemporal elements. The non-neuronal components—driven by artifacts such as movement, breathing, vascular pulsation, etc.—were identified based on their distribution in frequency (e.g., signal dominated by high frequencies) and space (e.g., signal originating outside the head) and removed. We observed 12 spatially independent neuronal components, whose time courses clustered into five groups; they were correlated within groups and anticorrelated/or less correlated between them, suggesting different functional roles. The spatial distribution revealed that the individual components clustered into five spatially distinct brain networks (Fig. S1). Subsequently, single-subject ICAs were also performed to calculate the cross-subject correlation within each of these networks. The five networks were identified in each participant's individual ICA. The time course of the component explaining the most variance from each network was correlated with the time course of the homologous ICA component in corresponding leave-one-out ICA (i.e., of the group minus that individual). A highly significant cross-subject correlation was observed for each network: *auditory*, $t(11) = 43.1$; $P < 0.00001$; *visual*, $t(11) = 11.9$; $P < 0.00001$; *frontoparietal*, $t(11) = 13.2$; $P < 0.00001$; *motor*, $t(11) = 4.5$; $P < 0.001$; and *precuneus*, $t(11) = 8$; $P < 0.00001$.

Model-Based and Data-Driven Analyses of fMRI Time Series. Based on the stereotypical brain activity observed in healthy participants during movie viewing, a model of healthy brain function could be generated against which preserved brain function in individual patients could be tested. As robustness at the single-subject level is a determining criterion for any work with individual brain-injured patients, initially, we tested whether activity in the rest of the group could predict that in each healthy participant. Single-subject analyses were focused on the three main networks, the auditory, visual, and frontoparietal, which were functionally critical for higher-order cognition during movie viewing. For each of these networks, 12 leave-one-out Tensor ICA analyses were performed, where each participant was, in turn, left out of the ICA analysis. Thus, the time course of each network in the participant subgroups was identified. Each network's time course (derived from the ICA of the group minus one participant) was then used as a regressor in the SPM data model of the participant not included in the ICA analysis. Twelve such SPM analyses were performed for each network.

Similarity of Executive Networks Revealed by the Movie Analysis, Behavioral Testing, and Large-Scale Metaanalysis. Initially, we calculated the pairwise similarity of the frontoparietal network elicited by movie viewing and the frontoparietal networks reflecting performance of the executive tasks. Their patterns were found to be highly similar to one another [Fig. S2; $r(48) = 0.31–0.44$; both pairs $P < 0.05$]. Subsequently, to demonstrate that the frontoparietal network revealed by each of the three tasks (i.e., movie viewing, dual task, and suspense rating) mapped directly onto the "canonical" frontoparietal network that has been repeatedly implicated in executive function, we obtained an independent localization of the executive network by using Neurosynth, a platform for large-scale metaanalysis of fMRI data from published studies (http://neurosynth.org/). Pairwise comparison between this executive network and the frontoparietal activation patterns in each of the three tasks in our study revealed that all three were statistically similar to the canonical executive network [Fig. S2; $r(48) = 0.49–0.59$; all $P < 0.001$]. Together, these results supported the primary results reported in the manuscript and, similarly, suggested that the movie-driven frontoparietal activation and the frontoparietal networks revealed by the behavioral tasks did indeed reflect the executive processes engaged during movie viewing. Finally, the spatial variability of the frontoparietal network across individuals was quantified with a leave-one-out analysis, where each individual's activation pattern was compared with that of the rest of the group. Individual frontoparietal networks were found to be highly similar to one another [$r(48) = 0.78–0.91$; all $P < 0.0001$].

Comparison of Brain Activity in Patients and Healthy Participants. In the previous three experiments with healthy participants we generated a model of healthy brain function during movie viewing against which preserved brain function in individual patients could be tested. This novel approach for directly predicting any given patient's brain activity from the time course of brain activity in healthy participants initially relies on the temporal similarity of the activity patterns to identify homologous processes in the two groups. Subsequently, the spatial extent of regional activity in the two groups is compared to interpret their functional correspondence. Slight differences in localization are expected not only due to differences in any given patient's morphological organization (e.g., widespread atrophy, enlarged ventricles, etc.) compared with controls, but also due to the normal anatomical variation observed even among individual healthy participants.

SI Results

The SART operates on the principle that insufficient attention to a task can result in slips of action as automatic, unintended action sequences are triggered inappropriately. These automatic actions result in performance errors that are detectable in the SART reaction times. In particular, a shortening of SART reaction times indicates a decrement in executive control or, conversely, an increment in response automaticity. Moreover, a shortening reaction time predicts an increased likelihood of a subsequent incorrect response to a "no go" digit and correlates with electrophysiological measures of waning attention. *Group-level analyses.* Group-averaged ($n = 19$) SART performance followed the canonical pattern. Specifically, reaction times in trials immediately preceding an incorrect button-press response (i.e., to a "no go" trial) were significantly shorter than those immediately preceding correctly withheld responses [$t(18) = 4.37$; $P < 0.0005$], suggesting that errors were due to lapses of attention (failure to inhibit a response to a "no go" trial), which may be driven by the simultaneous movie viewing. *Single-subject analyses*. Four out of nineteen of the participants did not show a SART effect in reaction times, whereas 15/19 showed both a SART effect ($P < 0.05$) and over 70% accuracy (1/15 had >71% accuracy; 14/15 had >78% accuracy) in the postmovie questionnaire. The reaction times of those participants (15/27) who were deemed to have correctly performed both components of the dual task were included in the fMRI analysis.

1. Giacino JT, Kalmar K, Whyte J (2004) The JFK coma recovery scale-revised: Measurement characteristics and diagnostic utility. *Arch Phys Med Rehabil* 85(12):2020–2029.
2. D'Esposito M, et al. (1995) The neural basis of the central executive system of working memory. *Nature* 378(6554):279–281.
3. Robertson IH, Manly T, Andrade J, Baddeley BT, Yiend J (1997) 'Oops!': Performance correlates of everyday attentional failures in traumatic brain injured and normal subjects. *Neuropsychologia* 35(6):747–758.
4. Whyte J, Grieb-Neff P, Gantz C, Polansky M (2006) Measuring sustained attention after traumatic brain injury: Differences in key findings from the sustained attention to response task (SART). *Neuropsychologia* 44(10):2007–2014.
5. Manly T, Robertson IH, Galloway M, Hawkins K (1999) The absent mind: Further investigations of sustained attention to response. *Neuropsychologia* 37(6):661–670.
6. Datta A, et al. (2007) The p300 as a marker of waning attention and error propensity. *Comput Intell Neurosci* 2007:1–9.
7. Peigneux P, et al. (2006) Offline persistence of memory-related cerebral activity during active wakefulness. *PLoS Biol* 4(4):e100.
8. Calhoun VD, et al. (2002) Different activation dynamics in multiple neural systems during simulated driving. *Hum Brain Mapp* 16(3):158–167.
9. Smith SM, et al. (2009) Correspondence of the brain's functional architecture during activation and rest. *Proc Natl Acad Sci USA* 106(31):13040–13045.

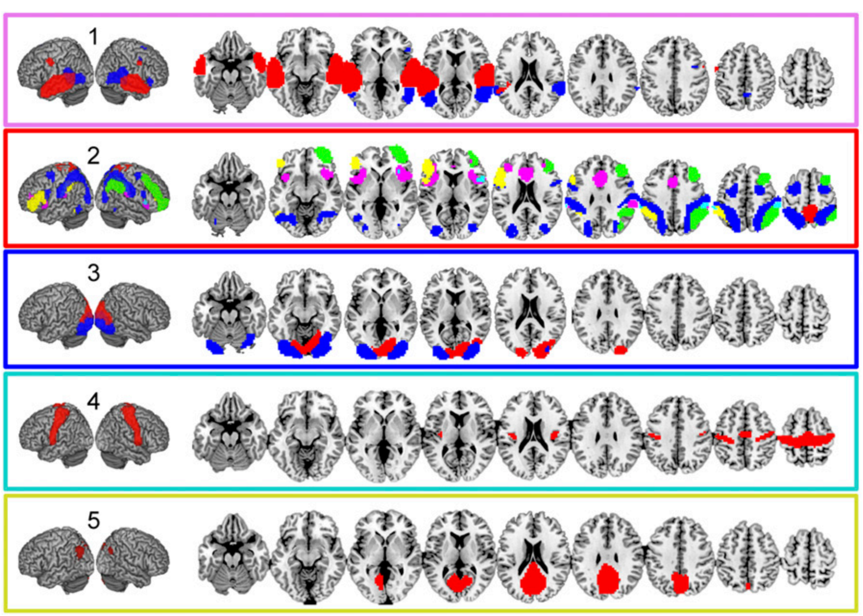

Fig. S1. Spatial clustering of independent components (IC) in healthy participants. The spatial distribution of the individual ICs revealed clustering into five spatially distinct functional brain networks, color-coded according to the respective grouping in the correlation matrix (Fig. 2): (1) auditory, (2) frontoparietal, (3) visual, (4) motor, and (5) precuneus. From left to right: each network is displayed on the lateral cortical surface bilaterally and on nine horizontal (ventral to dorsal) slices.

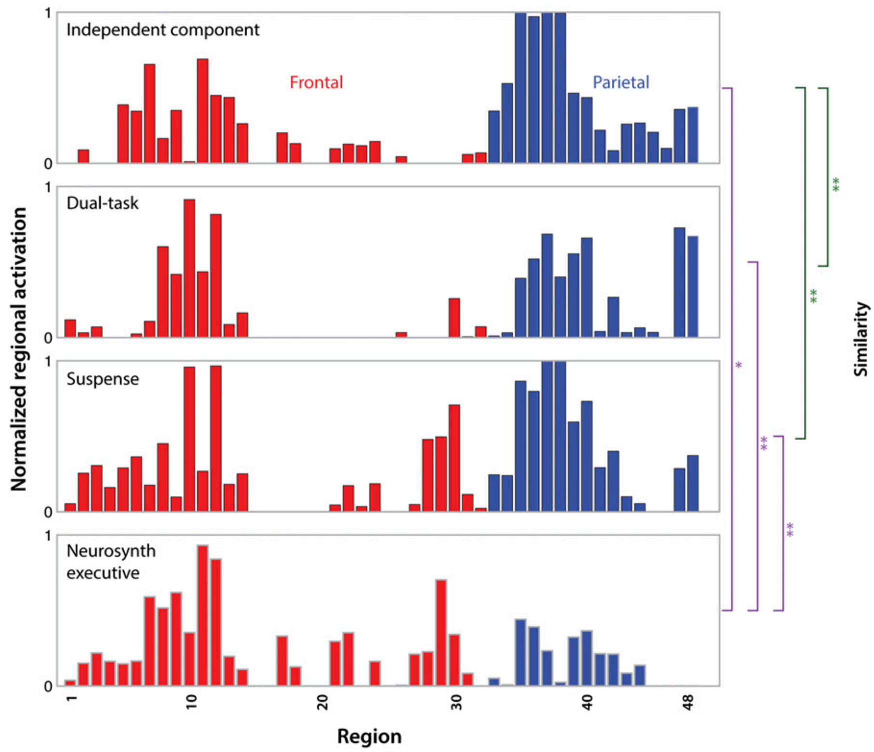

Fig. S2. Executive networks revealed by the movie analysis, behavioral testing, and large-scale metaanalysis. From *Top* to *Bottom*, the frontoparietal activation patterns are shown for the independent component of the movie fMRI data, the correlation with the dual-task performance, the correlation with the suspense ratings, and the executive network defined by the Neurosynth metaanalysis. Each bar represents the normalized regional activation in one of 48 regions, providing complete cover of the frontal (red) and parietal (blue) lobes (Harvard–Oxford atlas, http://fsl.fmrib.ox.ac.uk/fsl/fslwiki/Atlases). A similar subset of regions within the frontal and parietal lobes are activated by each different task: movie viewing, dual task, and suspense rating. Pairwise similarity comparisons between frontoparietal networks activated by the different tasks were calculated as the correlation between each pair of activation patterns. The frontoparietal activation patterns revealed by the dual task and the suspense ratings were significantly similar to that observed in the ICA of the movie data. Moreover, the frontoparietal activation patterns from the three tasks were statistically similar to the canonical executive network (Neurosynth). Significance values are shown to the *Right*: *, $P < 0.05$; **, $P < 0.01$. The numbers from left to right on the *x* axis label the 48 regions: 1. Left Frontal Pole; 2. Right Frontal Pole; 3. Left Insular Cortex; 4. Right Insular Cortex; 5. Left Superior Frontal Gyrus; 6. Right Superior Frontal Gyrus; 7. Left Middle Frontal Gyrus; 8. Middle Frontal Gyrus; 9. Left Inferior Frontal Gyrus, pars triangularis; 10. Right Inferior Frontal Gyrus, pars triangularis; 11. Left Inferior Frontal Gyrus, pars opercularis; 12. Right Inferior Frontal Gyrus, pars opercularis; 13. Left Precentral Gyrus; 14. Right Precentral Gyrus; 15. Left Frontal Medial Cortex; 16. Right Frontal Medial Cortex; 17. Left Juxtapositional Lobule Cortex (formerly Supplementary Motor Cortex); 18. Right Juxtapositional Lobule Cortex (formerly Supplementary Motor Cortex); 19. Left Subcallosal Cortex; 20. Right Subcallosal Cortex; 21. Left Paracingulate Gyrus; 22. Paracingulate Gyrus; 23. Left Cingulate Gyrus, anterior division; 24. Right Cingulate Gyrus, anterior division; 25. Left Cingulate Gyrus, posterior division; 26. Right Cingulate Gyrus, posterior division; 27. Left Frontal Orbital Cortex; 28. Frontal Orbital Cortex; 29. Left Frontal Operculum Cortex; 30. Right Frontal Operculum Cortex; 31. Left Central Opercular Cortex; 32. Right Central Opercular Cortex; 33. Left Postcentral Gyrus; 34. Right Postcentral Gyrus; 35. Left Superior Parietal Lobule; 36. Right Superior Parietal Lobule; 37. Supramarginal Gyrus, anterior division; 38. Right Supramarginal Gyrus, anterior division; 39. Left Supramarginal Gyrus, posterior division; 40. Right Supramarginal Gyrus, posterior division; 41. Left Angular Gyrus; 42. Right Angular Gyrus; 43. Left Precuneous Cortex; 44. Right Precuneous Cortex; 45. Left Cuneal Cortex; 46. Right Cuneal Cortex; 47. Left Parietal Operculum Cortex; 48. Right Parietal Operculum Cortex.